

Received July 29, 2020, accepted August 13, 2020, date of publication August 17, 2020, date of current version August 27, 2020.

Digital Object Identifier 10.1109/ACCESS.2020.3017148

# HARQ Assisted Short-Packet Communications for Cooperative Networks Over Nakagami- $m$ Fading Channels

YUCUI YANG<sup>1,2</sup>, YI SONG<sup>ID 1,2,3</sup>, AND FENGLIAN CAO<sup>1</sup>

<sup>1</sup>School of Physics and Electronic Electrical Engineering, Huaiyin Normal University, Huai'an 223001, China

<sup>2</sup>Jiangsu Province Key Construction Laboratory of Modern Measurement Technology and Intelligent System, Huai'an 223300, China

<sup>3</sup>College of Communications Engineering, Army Engineering University of PLA, Nanjing 210007, China

Corresponding author: Yucui Yang (htcyyc@163.com)

**ABSTRACT** Considering the coverage and short-packet communication requirements, this paper proposes a hybrid automatic repeat request (HARQ) assisted short-packet communications for cooperative Internet of Things (IoT) networks, where the signals are transmitted through short-packets. Since the short-packet communications will bring a higher packet error rate than long-packet communications, HARQ is adopted to improve transmission reliability by allowing retransmit the signals which cannot be detected correctly. For lighting the burden of the transmitter, the retransmitted signals are only sent from the relay. According to the detection capability of the user, selection combining (SC) scheme and maximum ratio combining (MRC) scheme are designed to detect the multiple transmitted signals. Besides, a set of closed-form expressions of the average packet error rate (APER) and effective throughput (ET) are derived over Nakagami- $m$  channels in the proposed SC and MRC schemes. For providing more insights into system performance, the asymptotic results are also provided. Simulation results demonstrate that HARQ will significantly improve reliability and transmission efficiency. Also, the MRC scheme outperforms the SC scheme in terms of APER and ET metrics, however, when the transmit power at the relay is high enough or the packet length is big enough, they achieve nearly the same performance.

**INDEX TERMS** Hybrid automatic repeat request, short-packet communications, cooperative Internet of Things.

## I. INTRODUCTION

With the development of the 5G and beyond 5G networks, Internet of Things (IoT) is coming to provide ubiquitous connectivity for smart office, smart industry, intelligent transportation, and so on [1]–[3]. For providing the ubiquitous connectivity, enhancing coverage becomes an important task in the development of IoT [4]. In this context, cooperative IoT utilizing relays for cooperating transmission emerges as a promising technique for enhancing coverage and realizing ubiquitous connectivity [5]. On the other hand, some critical IoT application scenarios, such as intelligent transportation system, demand the ultra-reliable and low-latency communications (URLLC), where the transmission delay is the key to realize the real-time control [6]. The transmission delay

is mainly caused by long packet. Supporting short-packet communications may reduce the delay significantly. Besides, in the sensor networks, the sensing data usually contains several bits and only needs a short-packet for transmission. Thus, short-packet communications are an inherent characteristic of IoT.

Recently, cooperative technology has been applied to IoT for enhancing coverage [7]–[13]. Chen *et al.* [9] considered an IoT network where an untrusted relay is utilized for improving transmission reliability. For avoiding traffic congestion and huge energy consumption, a relay assisted Device-to-device (D2D) system is employed into cellular IoT and network resources are optimally allocated [10]. Zhang *et al.* [11] aimed to many-to-many-to-one Internet of things (IoT) networks and designed a joint thing and relay selection criteria for balancing the performance and fairness. Considering the limited power in IoT, an energy harvesting

The associate editor coordinating the review of this manuscript and approving it for publication was Thanh Ngoc Dinh <sup>ID</sup>.

IoT system was proposed in [12], where relays are utilized to help the base station transmits signals to IoT devices. Besides, Shabbir *et al.* [13] considered a full-duplex relay with energy harvesting capability and proposed amplifying and forward (AF), and decode and forward (DF) relaying protocols for IoT networks. The above analysis shows that relay plays an important role in IoT for improving network capability.

Short-packet communications are widely existing in multiple IoT applications and considering the finite packet-length coding is realistic for real communication systems [14]–[16]. Chen *et al.* [17] proposed a wireless-powered IoT network with finite packet-length coding, where the effective-throughput (ET) and effective-amount-of-information are adopted as performance metrics and maximized by optimizing the delay and packet error rate. An enhanced random access scheme with short-packet communications was designed to support cellular IoT communications and the results shown that the proposed scheme can meet the reliability and low-latency requirements [18]. Considering the constrained resources in IoT, Wu *et al.* [19] adopted a short-packet for communications and an effective pilot-less one-shot transmission scheme was designed.

According to the state-of-art of cooperative IoT and short-packet communications, the finite packet coding will bring a higher packet error rate and reduce reception reliability. For enhancing transmission efficiency, a cooperative IoT protocol is proposed in [20], where the average throughput is optimized by designing effective optimal and suboptimal maximization methods. In a simultaneous wireless information and power transfer (SWIPT) assisted cooperative network, the transmission reliability performance is optimized by the optimal selection of SWIPT parameters [21]. Reference [22] investigated the blocklength-limited performance of a relaying system where the introduced weight factor is optimized to improve throughput and effective capacity. The authors in [23] studied the outage probability and the throughput of amplify-and-forward relay networks with finite block-length codes. The source and the destination nodes in the networks are assumed to have constrained energy supply, and the time switching relaying and the power splitting relaying protocols are considered for energy and information transfer.

On the one hand, hybrid automatic repeat request (HARQ) is adopted in multiuser multiple-input-multiple-output (MIMO) system and maximal ratio combining (MRC) scheme is employed [24]. On the other hand, HARQ is also recruited for improving the transmit reliability in short-packet communications [25]–[27]. An incremental redundancy HARQ scheme is adopted in [25] to reduce outage probability and improve throughput. Considering the outage performance in the energy constrained system, Makki *et al.* [26] proposed a wireless energy and information transfer scheme with retransmissions; results show that the retransmission protocol reduces outage probability. For reducing the delay bring by HARQ, a fast HARQ protocol is designed in [27] and the delay is reduced by 27, 42, 52 and 60 % when 2, 3, 4 and 5 transmission rounds are adopted, respectively.

In this paper, we further investigated the performance of short-packet communications. Different from the scheme in references [20]–[23], we adopt an HARQ technique to improve the reliability performance in short-packet communications. Also, different from [25]–[27], cooperative techniques are employed in this paper to enhance coverage. Although the performance of cooperative networks with HARQ in infinite packet communications has been investigated [28], [29], there are little studies about the combination of cooperative techniques and HARQ in short-packet communications, which may satisfy the low-complexity and large coverage requirements of IoT. The main contributions are summarized as follows.

- We consider a cooperative IoT network where a relay assists to transmit the signals conveyed on the short-packet. For mitigating the packet error caused by short-packet communications, an HARQ scheme is employed, where the signal will be retransmitted only from the relay to lighten the burden of the transmitter when the user cannot detect its message correctly.
- According to the characteristics of HARQ, the selection combining (SC) scheme and MRC scheme are designed. In the SC scheme, the user abandons the received signal when it is decoded with error; while in the MRC scheme, the user saves every transmission and combines them by MRC for detection.
- A generalized Nakagami- $m$  fading channel is considered in the networks and the closed-form expressions for the average packet error rate (APER) and ET are derived in both SC and MRC schemes. Besides, the asymptotic results of APER and ET when the transmit power at the transmitter and relay tends to infinite are analyzed.
- Simulations are conducted and the results show that HARQ is beneficial to improve reliability and transmission efficiency; in addition, the MRC scheme outperforms SC scheme in terms of APER and ET; furthermore, the packet-length can be optimized for achieving higher ET.

The rest of the paper is arranged as follows. The network model and the transmission schemes are introduced in Section II. The closed-form expressions for the APER and ET in SC and MRC schemes are derived at Section III and Section IV, respectively. Next, in Section V, Simulations are conducted to verify the analysis results and some insights into system characteristics are provided. Finally, Section VI concludes the paper.

## II. NETWORK MODEL AND TRANSMISSION SCHEMES

### A. NETWORK MODEL

As shown in Fig. 1, we consider a cooperative network where a decode-and-forward relay denoted as  $R$  cooperates with the transmitter  $T$  for providing reliable short-packet communications for the user denoted as  $U$ . The transmitter conveys the short-packet (e.g., packet size  $\leq 10^3$  bytes [30]) to the user. We assume there no direct channel between the transmitter

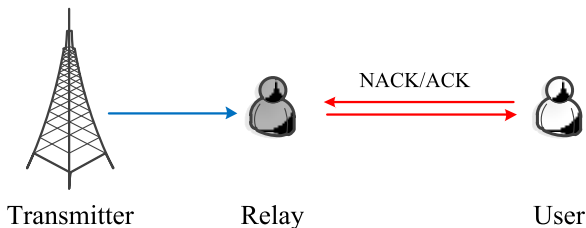


FIGURE 1. Illustration of the network model.

and the user [31]. Therefore, reliable communications have to depend upon a relay. Due to the short-packet communications, the applications of effective channel coding schemes, such as Low-density parity-check code and turbo code, are limited. Thus, reliable communications cannot always be guaranteed even in the high transmit power region. For ensuring the reliable communication of the user, HARQ is recruited to retransmit the signal that failed to be decoded by the user. When the user decodes the intended message with error, it feeds back a NACK for requesting retransmission; otherwise, it feeds back an ACK. To reduce the burden of the transmitter, the retransmitted signals are only sent by the relay. When the relay receives an ACK or the number of transmission rounds goes to the maximum allowed number  $L$ , the relay stops retransmission [32], [33].

The block Nakagami- $m$  fading is adopted to model the channels in the wireless networks, which is a generalized model and can be degraded to Rayleigh fading and Rician fading by choosing different fading parameters [34]. The channel between the transmitter and relay is denoted as  $h_R$  with mean  $\Omega_R$  and fading parameter  $m_R$ . In  $j$ th transmission, the channel between the relay and the user is denoted as  $h_U^j$  with mean  $\Omega_U$  and fading parameter  $m_U$ . All the nodes in the network are assumed to be equipped with a single antenna and working under half-duplex mode. The AWGN powers at the receivers are  $\sigma^2$ . The specific transmission scheme is detailed as follows.

Transmitter sends signal  $x_U$  with  $B$  information bits over a short-packet with packet length  $N$  to the relay and the code rate  $R_T = B/N$ . The signal to noise ratio (SNR) is denoted as

$$\gamma_R = \frac{P_T |h_R|^2}{\sigma^2}, \tag{1}$$

where the  $P_T$  is the transmit power of the transmitter.

In the short packet communications, for the fixed code rate  $R_T$ , the resulting packet error rate (PER) is approximated by [35]

$$\varepsilon_R \approx Q \left( \ln 2 \sqrt{\frac{N}{V(\gamma_R)}} (\log_2 (1 + \gamma_R) - R_T) \right), \tag{2}$$

where  $Q^{-1}(\cdot)$  is the inverse of the Gaussian Q-function  $Q(x) = \int_x^\infty \frac{1}{\sqrt{2\pi}} e^{-\frac{t^2}{2}} dt$  and  $V(x) = 1 - (1+x)^{-2}$ . Because (2) provides a tight approximation, in the following analysis, the “ $\approx$ ” is replaced by “ $=$ ”.

When the relay failed to decode  $x_U$ , packet error is inevitable; otherwise, the relay will send the signal to the User. When the user decoded  $x_U$  with error, the relay retransmits the signal until the user receives the message correctly or the number of transmission rounds goes to  $L$ . Two schemes can be adopted to utilize the retransmitted signals, which are detailed as follows.

**B. SC SCHEME**

In the SC scheme, the user will abandon the received signal when it is decoded with errors and a NACK is feedback to the relay. Only the signal decoded without error is selected. In the  $j$ th transmission, the SNR received at the user is given by

$$\gamma_S^j = \frac{P_R |h_U^j|^2}{\sigma^2}, \tag{3}$$

where  $P_R$  is the transmit power of the relay. Thus, in the  $j$ th transmission the PER is expressed as

$$\varepsilon_S^j = Q \left( \ln 2 \sqrt{\frac{N}{V(\gamma_S^j)}} (\log_2 (1 + \gamma_S^j) - R_T) \right). \tag{4}$$

**C. MRC SCHEME**

In the MRC scheme, the user will save the received signals when they are decoded with errors and combine the retransmitted signals with MRC. After  $l$  transmissions, the SNR received at the user is given by

$$\gamma_M^l = \frac{P_R \sum_{j=1}^l |h_U^j|^2}{\sigma^2}. \tag{5}$$

Thus, after  $l$  transmissions the PER is expressed as

$$\varepsilon_M^l = Q \left( \ln 2 \sqrt{\frac{N}{V(\gamma_M^l)}} (\log_2 (1 + \gamma_M^l) - R_T) \right). \tag{6}$$

From (3) and (5), we can observe that the SNR achieved in the MRC scheme is higher than that in the SC scheme because every transmission is utilized by MRC. Thus, the MRC scheme may achieve better performance than the SC scheme. However, for providing an efficient combination by MRC, the user requires the perfect CSI, which results in the extra communication resource consumption.

**III. PERFORMANCE ANALYSIS OF THE SC SCHEME**

In this section, we adopt APER and ET as performance metrics for evaluating the reliability and efficiency of the proposed system. The closed-form expressions for APER and ET are derived in the SC scheme.

**A. AVERAGE PACKET ERROR RATE IN THE SC SCHEME**

When the user decodes its intended messages with error, it will request for retransmission, until the user correctly decodes  $x_U$  or the number of transmission rounds goes to

*L*. The packet error is inevitable when the relay cannot decode  $x_U$  correctly or the user still cannot obtain its intended messages after  $L$  transmissions. Thus, the APER in the SC scheme is given by

$$A_{per}^S = 1 - (1 - \Pr[\Phi_R]) \left( 1 - \Pr[\Phi_S^1, \dots, \Phi_S^j, \dots, \Phi_S^L] \right), \quad (7)$$

where  $\Phi_R$  and  $\Phi_S^j$  denote the event that the packet error occurs at the relay and the user in the  $j$ th transmission, respectively.

Due to the channels in different transmission rounds are independent, the APER can be further expressed as

$$A_{per}^S = 1 - (1 - E[\varepsilon_R]) \times \left( 1 - E[\varepsilon_S^1] \times \dots \times E[\varepsilon_S^j] \times \dots \times E[\varepsilon_S^L] \right). \quad (8)$$

where  $E[x]$  is the expectation operation.

Before deriving the closed-form expression for  $A_{per}^S$ , we first deriving the closed-form expression for  $E[\varepsilon_R]$  which is given in the following **Lemma**.

**Lemma 1:** The closed-form expression for  $E[\varepsilon_R]$  is expressed as

$$\begin{aligned} E[\tilde{\varepsilon}_R] &= \left( \frac{1}{2} + g\sqrt{N}h \right) F_{|h_R|^2} \left( \frac{q}{\rho_T} \right) \\ &+ \left( \frac{1}{2} - g\sqrt{N}h \right) F_{|h_R|^2} \left( \frac{p}{\rho_T} \right) - \frac{g\rho_T\sqrt{N}}{\Gamma(m_R)} \left( \frac{m_R}{\Omega_R} \right)^{-1} \\ &\times \left( \Upsilon \left( m_R + 1, \frac{qm_R}{\rho_T\Omega_R} \right) - \Upsilon \left( m_R + 1, \frac{pm_R}{\rho_T\Omega_R} \right) \right), \quad (9) \end{aligned}$$

where  $h = 2^{R_T} - 1$ ,  $g = (2\pi(2^{2R_T} - 1))^{-\frac{1}{2}}$ ,  $p = h - \frac{1}{2}g^{-1}N^{-\frac{1}{2}}$ ,  $q = h + \frac{1}{2}g^{-1}N^{-\frac{1}{2}}$ ,  $\Upsilon(\alpha, x) = \int_0^x e^{-t}t^{\alpha-1}dt$ ,

$$\rho_T = \frac{P_T}{\sigma^2}, \text{ and } F_{|h_R|^2}(x) = 1 - \sum_{t=0}^{m_R-1} \left( \frac{m_R x}{\Omega_R} \right)^t \frac{1}{t!} e^{-\frac{m_R x}{\Omega_R}}.$$

*Proof:* See Appendix A.

From (2) and (4), we can find that  $\varepsilon_R$  and  $\varepsilon_S^j$  have a similar expression. Thus, following the steps in deriving  $E[\tilde{\varepsilon}_R]$ , we can obtain the closed-form expression for  $E[\tilde{\varepsilon}_S^j]$  by replacing  $m_R$  by  $m_U$ , replacing  $\Omega_R$  by  $\Omega_U$ , and replacing  $\rho_T$  by  $\rho_R$  in (9). The closed-form expression for  $E[\tilde{\varepsilon}_S^j]$  is expressed as

$$\begin{aligned} E[\tilde{\varepsilon}_S^j] &= \left( \frac{1}{2} + g\sqrt{N}h \right) F_{|h_U|^2} \left( \frac{q}{\rho_R} \right) \\ &+ \left( \frac{1}{2} - g\sqrt{N}h \right) F_{|h_U|^2} \left( \frac{p}{\rho_R} \right) - \frac{g\rho_R\sqrt{N}}{\Gamma(m_U)} \left( \frac{m_U}{\Omega_U} \right)^{-1} \\ &\times \left( \Upsilon \left( m_U + 1, \frac{qm_U}{\rho_R\Omega_U} \right) - \Upsilon \left( m_U + 1, \frac{pm_U}{\rho_R\Omega_U} \right) \right), \quad (10) \end{aligned}$$

where  $F_{|h_U|^2}(x) = 1 - \sum_{t=0}^{m_U-1} \left( \frac{m_U x}{\Omega_U} \right)^t \frac{1}{t!} e^{-\frac{m_U x}{\Omega_U}}$ , and  $\rho_R = \frac{P_R}{\sigma^2}$ .

From (9) and (10), we can find that  $E[\tilde{\varepsilon}_R]$  and  $E[\tilde{\varepsilon}_S^j]$  are decreasing function about transmit power. When  $\{P_T, P_R\} \rightarrow 0$ ,  $E[\tilde{\varepsilon}_R] = E[\tilde{\varepsilon}_S^j] = 1$ , and when  $\{P_T, P_R\} \rightarrow \infty$ ,  $E[\tilde{\varepsilon}_R] = E[\tilde{\varepsilon}_S^j] = 0$ .

Due to the channels in different transmission rounds are independent and identically distributed (i.i.d.),  $E[\tilde{\varepsilon}_S^1] = E[\tilde{\varepsilon}_S^j] = E[\tilde{\varepsilon}_S^L]$ . The closed-form expression for the APER in the SC scheme is given by

$$A_{per}^S = 1 - (1 - E[\varepsilon_R]) \left( 1 - \left( E[\varepsilon_S^j] \right)^L \right), \quad (11)$$

where  $E[\tilde{\varepsilon}_R]$  and  $E[\tilde{\varepsilon}_S^j]$  are given in (9) and (10), respectively.

From (11), we can observe that increasing  $L$  will reduce APER, which shows that HARQ is beneficial to reliable transmission. Besides, when  $L$  tends to infinite,  $A_{per}^S = E[\varepsilon_R]$ , which demonstrates that the reliability performance is determined by the detection ability of the relay.

### B. EFFECTIVE THROUGHPUT IN THE SC SCHEME

Although HARQ improves transmission reliability, the same message being transmitted multiple times will degrade the efficiency. Effective throughput is adopted to evaluate the transmission efficiency of the HARQ system. Different from [36], motivated by the total probability formula, the EST is defined as [33]

$$\eta_S = \sum_{l=1}^L \frac{R_T}{l} (1 - \Pr[\Phi_R]) \Pr[\Phi_S^1, \dots, \Phi_S^j, \dots, \bar{\Phi}_S^l], \quad (12)$$

where  $\bar{\Phi}_S^l$  denotes the event that the user correctly decodes its intended message in the  $l$ th transmission. (12) shows the sum of average transmission rate in a successful transmission process multiplying its corresponding probability.

Due to the channels in different transmission round is i.i.d., (12) can be further expressed as

$$\eta_S = \sum_{l=1}^L \frac{R_T}{l} (1 - E[\varepsilon_R]) \left( E[\varepsilon_S^j] \right)^{l-1} \left( 1 - E[\varepsilon_S^j] \right), \quad (13)$$

where  $E[\tilde{\varepsilon}_R]$  and  $E[\tilde{\varepsilon}_S^j]$  are given in (9) and (10), respectively.

From (13), we can deduce that increasing  $L$  will increase ET because every item in the sum function is positive. It demonstrates that HARQ benefits to the transmission efficiency. However, for a large  $l$  the item in the sum function is small, which shows that HARQ is limited for improving transmission efficiency.

### IV. PERFORMANCE ANALYSIS OF THE MRC SCHEME

Similar to the SC scheme, APER and ET are also adopted as the metrics in the MRC scheme for evaluating the reliability and efficiency performance, respectively.

**A. AVERAGE PACKET ERROR RATE IN THE MRC SCHEME**

In the MRC scheme, when the user cannot decode its intended message correctly, a NACK will be fed back for requesting retransmission. The user will combine the original and every retransmitted signal by MRC. After  $L$  times of transmissions, the user still cannot obtain its messages correctly, The APER in the MRC scheme is given by the packet will be received with errors.

$$A_{per}^M = 1 - (1 - \Pr[\Phi_R]) \left(1 - \Pr[\Phi_M^L]\right), \quad (14)$$

where  $\Phi_M^L$  represents the event that after  $L$  times of transmission the user still cannot obtain its message correctly in the MRC scheme.

Similar to the SC scheme, (14) can be further expressed as

$$A_{per}^M = 1 - (1 - E[\varepsilon_R]) \left(1 - E[\varepsilon_M^L]\right), \quad (15)$$

where  $E[\varepsilon_M^L]$  is the average PER after  $L$  times of transmission.

Before deriving the closed-form expression for  $A_{per}^M$ , we first derive the closed-form expressions for  $E[\varepsilon_M^l]$ , which is given in the following **Lemma**.

*Lemma 2:* The closed-form expression for  $E[\varepsilon_M^l]$  is given by

$$\begin{aligned} E[\varepsilon_M^l] &= \left(\frac{1}{2} + g\sqrt{N}h\right) F_{\sum_{j=1}^l |h_U^j|^2} \left(\frac{q}{\rho_R}\right) \\ &+ \left(\frac{1}{2} - g\sqrt{N}h\right) F_{\sum_{j=1}^l |h_U^j|^2} \left(\frac{p}{\rho_R}\right) - \frac{g\rho_R\sqrt{N}}{\Gamma(m_U l)} \left(\frac{m_U}{\Omega_U}\right)^{-1} \\ &\times \left(\Upsilon\left(m_U l + 1, \frac{qm_U}{\rho_R \Omega_U}\right) - \Upsilon\left(m_U l + 1, \frac{pm_U}{\rho_R \Omega_U}\right)\right), \quad (16) \end{aligned}$$

where  $F_{\sum_{j=1}^l |h_U^j|^2}(x) = 1 - \sum_{i=0}^{m_U l - 1} \left(\frac{m_U x}{\Omega_U}\right)^i \frac{1}{i!} e^{-\frac{m_U x}{\Omega_U}}$ .

Similar to the SC scheme,  $E[\varepsilon_M^l]$  also is a decreasing function about transmit power  $P_R$ . When  $P_R \rightarrow 0$ ,  $E[\varepsilon_M^l] = 1$ , and when  $P_R \rightarrow \infty$ ,  $E[\varepsilon_M^l] = 0$ . Replacing  $l$  by  $L$  in (16), the closed-form expression for  $E[\varepsilon_M^L]$  is obtained. Substituting  $E[\varepsilon_R]$  and  $E[\varepsilon_M^L]$  into (15), the closed-form expression for the APER in the MRC scheme is obtained.

From (16) we can find that  $E[\varepsilon_M^l]$  decreases with the increase of  $l$ . According to (15), increase  $l$  will reduce APER in the MRC scheme. Similar to the SC scheme, HARQ is also beneficial to the reliable transmissions in the MRC scheme. In addition, when  $L$  tends to infinite,  $E[\varepsilon_M^L]$  tends to zero and  $A_{per}^M = E[\varepsilon_R]$ . It demonstrates that the MRC and SC schemes achieve the same reliability performance, because, in this case, the reliability performance is only determined by the relay.

**TABLE 1.** Table of parameters.

Parameter	value
Monte carlo simulations repeated	$10^5$ times
Fading means	$\Omega_R = -100dB,$ $\Omega_U = -110dB$
Fading parameters	$m_U = 3, m_R = 2$
The amount of information bits	$B = 500$
The length of the short-packet	$N = 100$
Noise power	$\sigma^2 = -121dBm$

**B. EFFECTIVE THROUGHPUT IN THE MRC SCHEME**

Similar to the SC scheme, in the SC scheme, we adopt ET to evaluate the transmission efficiency, which is expressed as

$$\eta_M = \sum_{l=1}^L \frac{R_T}{l} (1 - \Pr[\Phi_R]) \Pr[\Phi_S^{l-1}, \bar{\Phi}_S^l], \quad (17)$$

where  $\bar{\Phi}_M^l$  represents the event that after  $l$  times of transmissions the user decodes its intended message correctly.

Due to the independency between every transmission, (17) can be further expressed as

$$\eta_M = \sum_{l=1}^L \frac{R_T}{l} (1 - E[\varepsilon_R]) E[\varepsilon_M^{l-1}] \left(1 - E[\varepsilon_M^l]\right), \quad (18)$$

where we define  $E[\varepsilon_M^0] = 1$ , and  $E[\varepsilon_M^{l-1}]$  can be obtained by replacing  $l$  by  $l - 1$  in (16).

Similar to the SC scheme, (18) also shows that increasing  $L$  will improve ET, which demonstrates that HARQ helps to improve transmission efficiency.

*Remark 1:* When  $P_T \rightarrow \infty$ , according to (11) and (15),  $A_{per}^S = (E[\varepsilon_S^j])^L$  and  $A_{per}^M = E[\varepsilon_M^L]$ . Besides, when  $P_T \rightarrow \infty$ , according to (13) and (18), the ETs in the SC and MRC schemes are degenerated as

$$\eta_S = \sum_{l=1}^L \frac{R_T}{l} (E[\varepsilon_S^j])^{l-1} \left(1 - E[\varepsilon_S^j]\right), \quad (19)$$

$$\eta_M = \sum_{l=1}^L \frac{R_T}{l} E[\varepsilon_M^{l-1}] \left(1 - E[\varepsilon_M^l]\right), \quad (20)$$

respectively. It shows that the APER and ET are only determined by the reception performance of the user.

On the other hand, according to (11), (13), (15), and (18), when  $P_R \rightarrow \infty$ ,  $A_{per}^S = A_{per}^M = E[\varepsilon_R]$  and  $\eta_S = \eta_M = R_T (1 - E[\varepsilon_R])$ . It shows the SC and MRC schemes achieve the same reliability and transmission efficiency, because when  $P_R \rightarrow \infty$ , the APER and ET are only determined by the reception performance of the relay without HARQ. Thus, both SC and MRC schemes obtain the same performance.

**V. NUMERICAL RESULTS**

In this section, numerical results are presented to verify our analysis and investigate the effects of the key parameters on

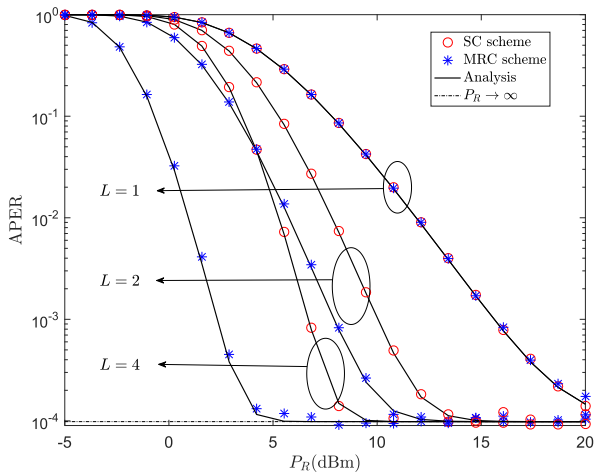


FIGURE 2. The APER versus  $P_R$  with  $P_T = 15\text{dBm}$ , in both SC and MRC schemes.

the system performance. Unless otherwise stated, part of the simulation parameters is given in Table 1, where the bit per channel use (BPCU) is used as the unit for transmission rate.

Fig. 2 plots the APER versus  $P_R$  in both SC and MRC scheme for  $P_T = 15\text{dBm}$  and different maximum transmission round  $L$ . Firstly, we can find that the simulation points match the analysis curves well, which demonstrates the correctness of the derivations. Secondly, the APER drops dramatically with the increase of  $P_R$  and finally tends to the asymptotic results. It shows that high transmit power at the relay benefits to the reliable transmission and when the power is higher enough, the APER is determined by the reception performance of the relay. When  $L = 1$ , the proposed schemes are degenerated to non-HARQ schemes and both SC and MRC schemes achieve the same reliability performance. Also, the APERs in both SC and MRC schemes decrease with the increase of  $L$ , which shows HARQ is a benefit to reliable transmission. Especially, we can find that the MRC scheme outperforms SC scheme because every transmission is utilized efficiently in the MRC schemes.

Fig. 3 depicts the APER versus  $P_T$  in the SC and MRC schemes for  $P_R = 4\text{dBm}$  and  $L = 3$ . We can obtain from Fig. 3 that the APER decreases with the increase of transmit power  $P_T$ , which demonstrates that high transmit power at the transmitter helps to reliable transmission. However, the APER cannot keep dropping with the increase of  $P_T$  and finally tends to a performance floor which is determined by the reception performance of the user. Fig. 3 also shows that the reliability performance achieved at the MRC scheme is better than that achieved at the SC scheme. Nevertheless, the performance gains in the MRC scheme is achieved at the cost of high resource consumption. When the fading parameters increase from 1 to 3, the APER decreases in both SC and MRC schemes, which shows that the stable channels are benefiting to reliable transmission.

Fig. 4 illustrates the APER versus packet-length  $N$  for  $P_R = 4\text{dBm}$  and  $P_T = 8\text{dBm}$  in both SC and MRC schemes. Different from Fig. 2 and Fig. 3, Fig. 4 shows that the curves

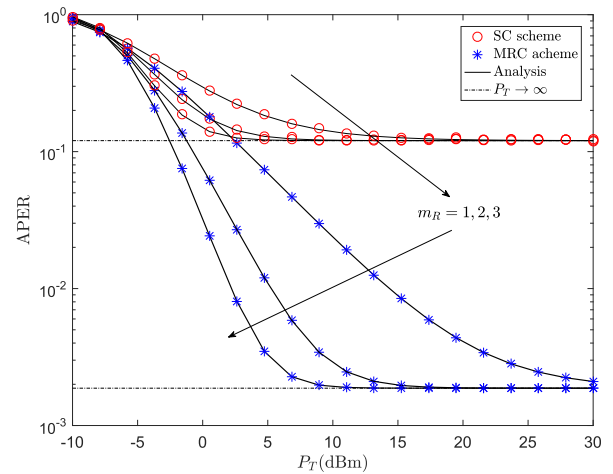


FIGURE 3. The APER versus  $P_T$  with  $P_R = 4\text{dBm}$  and  $L = 3$  in both SC and MRC schemes.

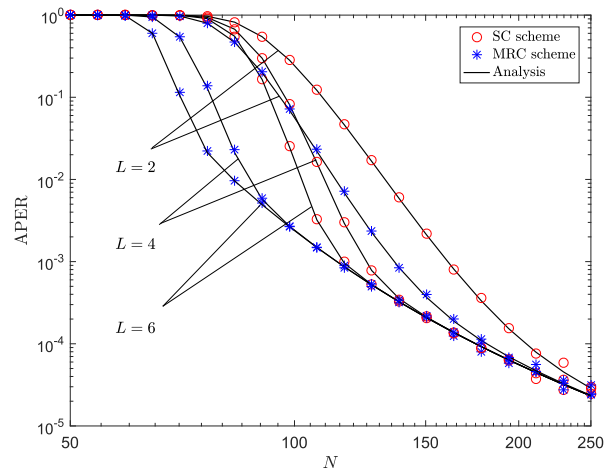


FIGURE 4. The APER versus  $N$  in both SC and MRC schemes for  $P_R = 4\text{dBm}$  and  $P_T = 8\text{dBm}$ .

of APER keep dropping with the increase of packet-length  $N$  in both SC and MRC schemes. This is because an increase of  $N$  will decrease the transmit rate resulting in the improvement of reliability. However, increasing  $N$  will also increase the transmit delay, which should be reasonably determined, especially when the system requires URLLC. We can also find that the MRC scheme outperforms the SC scheme for different  $L$ , but they achieve the same performance when the  $N$  is bigger enough. It can be explained that when  $N$  is big, only one transmission can satisfy the communication requirement and both SC and MRC schemes degenerate to the non-HARQ schemes. Thus, they achieve the same APER. Ultimately, we can observe that increase the maximum transmission round  $L$  will reduce APER, which also shows that HARQ benefits to reliable transmission. However, the  $L$  also should be determined carefully because a big  $L$  will bring a high transmission delay.

Fig. 5 plots the ET versus transmit power  $P_R$  for  $P_T = 4\text{dBm}$ , in both SC and MRC schemes. Firstly, we can observe from Fig. 5 that the ET increases rapidly with an increase of  $P_R$ . It demonstrates that high transmit power at the relay helps

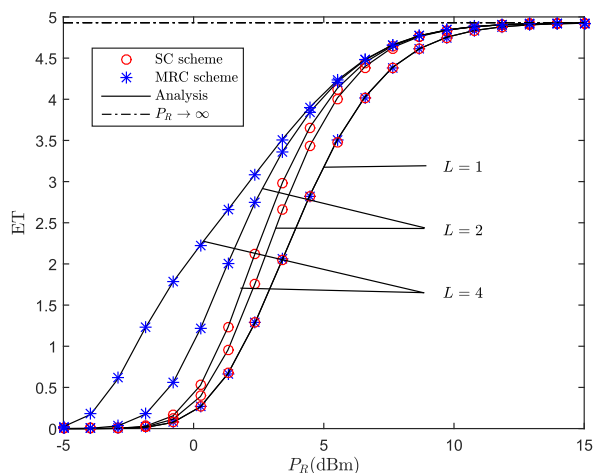


FIGURE 5. The ET versus  $P_R$  in both SC and MRC schemes for  $P_T = 4\text{dBm}$  and different  $L$ .

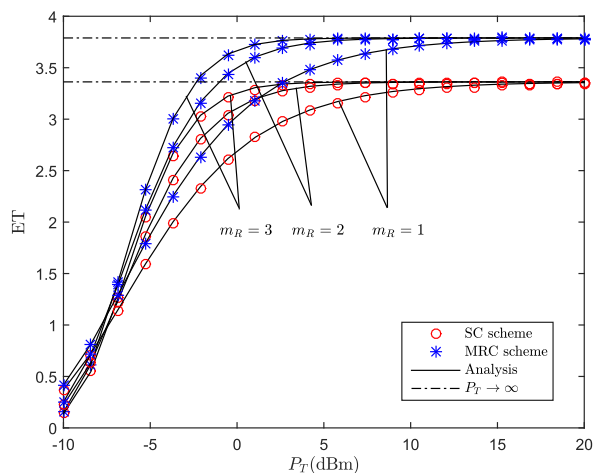


FIGURE 6. The ET versus  $P_T$  in the SC and MRC schemes for  $L = 4$  and  $P_R = 4\text{dBm}$ .

to improve transmission efficiency. However, when further improving  $P_R$ , the ETs in both SC and MRC schemes tend to the asymptotic results which are determined by the transmit power  $P_T$  at the transmitter. Besides, when  $L = 1$ , the proposed schemes are degenerated to non-HARQ scheme and achieve the worst performance when compared with the case of  $L = 2$  and  $L = 4$ , which shows that the proposed HARQ schemes benefit to transmission efficiency. It also shows that the MRC scheme outperforms the SC scheme in terms of ET because the MRC scheme saves every transmission for detection.

Fig. 6 depicts the ET versus  $P_T$  for  $L = 4$  and  $P_R = 4\text{dBm}$  in the SC and MRC schemes. As observed in Fig. 6, with an increase of  $P_T$ , the curves of ET increase in both SC and MRC schemes, and finally tend to their correspondence asymptotic results, which verifies the analysis results in the *remark 1*. Besides, we can find the MRC scheme strictly outperforms the SC scheme in different  $P_T$ . However, the SC scheme consumes fewer communication resources and can be applied to multiple scenarios with constrained resources. Furthermore, in the high transmit power region, when  $m_R$  increases from

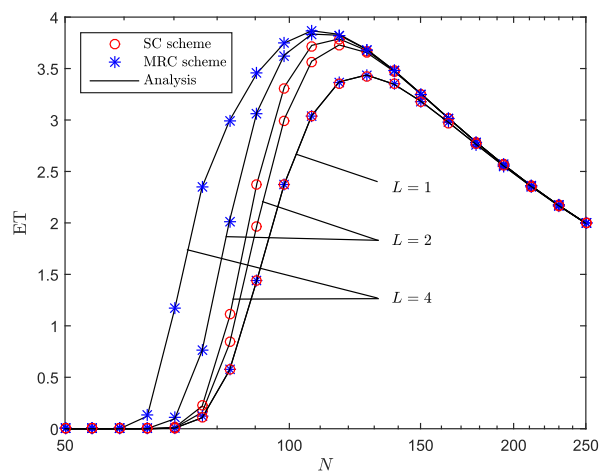


FIGURE 7. The ET versus  $N$  in the SC and MRC schemes for  $P_T = 8\text{dBm}$  and  $P_R = 4\text{dBm}$ .

1 to 3, i.e., the channel becomes stability, the ET improved in both SC and MRC schemes. On the contrary, in a low transmit power region, the variation of channels benefits to transmission efficiency. It demonstrates that the stability of channels can be utilized to improve transmission efficiency.

In Fig. 7, we plots the ET versus packet-length  $N$  with  $P_T = 8\text{dBm}$  and  $P_R = 4\text{dBm}$ , in the SC and MRC schemes. Firstly, we can observe that the ET first increases and then decreases with the increase of  $N$  in both SC and MRC schemes. It is because an increase of  $N$  will improve the transmission reliability but further increase  $N$  the transmit rate will decrease. When  $N$  is small, the reliability dominates the transmission efficiency, and increasing  $N$  will improve reliability and increase ET. When  $N$  is big enough, the transmission efficiency is dominated by the transmit rate, increasing  $N$  will decrease the transmit rate and deteriorate ET. It also shows that the packet-length  $N$  can be optimized for achieving higher ET. Besides, we can find that the ET is improved with the increase of maximum transmission round  $L$  for different  $N$ , which shows that the retransmission will improve transmission efficiency. We also find that the MRC scheme outperforms the SC scheme in different  $N$ , however, the performance in the MRC scheme is achieved at the cost of high resource consumption. It demonstrates that the performance and the cost should be jointly considered when choosing a proper scheme.

## VI. CONCLUSION

In this paper, we adopt HARQ for improving the short-packet communication performance of cooperative IoT networks. Both SC and MRC schemes are designed for detecting the multiple transmitted signals. We derived the closed-form expressions of the APER and ET in both SC and MRC schemes over Nakagami- $m$  fading channels. Results show that HARQ improves the reliability and transmission efficiency when compared with the non-HARQ scheme, and increasing the maximum transmission round  $L$  will further improve system performance. Besides, the performance

achieved in the MRC scheme is better than that in the SC scheme. However, the SC scheme consumes fewer communication resources and can be applied to multiple IoT applications. Furthermore, the fading parameters also have an important effect on system performance and when the channel becomes stable the system performance will be improved. Ultimately, the transmission efficiency can be improved by choosing a proper packet-length.

**APPENDIX A  
PROOF OF LEMMA 1**

Utilizing (2),  $\varepsilon_R$  can be approximated as [25]

$$\tilde{\varepsilon}_R = \begin{cases} 1, & \gamma_R \leq p \\ \frac{1}{2} - g\sqrt{N}(\gamma_R - h), & p < \gamma_R < q \\ 0, & \gamma_R \geq q. \end{cases} \quad (21)$$

Using (1) and (21), the average block error rate is expressed as

$$E[\tilde{\varepsilon}_R] = \int_0^\infty \tilde{\varepsilon}_R(\rho_T x) f_{|h_R|^2}(x) dx, \quad (22)$$

where  $f_{|h_R|^2}(x) = \left(\frac{m_R}{\Omega_R}\right)^{m_R} \frac{x^{m_R-1}}{\Gamma(m_R)} e^{-\frac{m_R x}{\Omega_R}}$  is the probability density function (PDF) of  $|h_R|^2$  [37], [38].

According to (21),  $E[\tilde{\varepsilon}_R]$  can be further expressed as

$$E[\tilde{\varepsilon}_R] = \int_{\frac{p}{\rho_T}}^{\frac{q}{\rho_T}} \left(\frac{1}{2} - g\sqrt{N}(\rho_T x - h)\right) f_{|h_R|^2}(x) dx + \int_0^{\frac{p}{\rho_T}} f_{|h_R|^2}(x) dx. \quad (23)$$

Substituting the PDF of  $|h_R|^2$  into (23), which can be expressed as

$$E[\tilde{\varepsilon}_R] = \left(\frac{1}{2} + g\sqrt{N}h\right) F_{|h_R|^2}\left(\frac{q}{\rho_T}\right) + \left(\frac{1}{2} - g\sqrt{N}h\right) F_{|h_R|^2}\left(\frac{p}{\rho_T}\right) - \left(\frac{m_R}{\Omega_R}\right)^{m_R} \frac{\rho_T \sqrt{N}}{\Gamma(m_R)} \times g \left( \int_0^{\frac{q}{\rho_T}} x^{m_R} e^{-\frac{m_R x}{\Omega_R}} dx - \int_0^{\frac{p}{\rho_T}} x^{m_R} e^{-\frac{m_R x}{\Omega_R}} dx \right). \quad (24)$$

Utilizing [39, eq.(3.351.1)],  $E[\tilde{\varepsilon}_R]$  is derived as (9).

**APPENDIX B  
PROOF OF LEMMA 2**

Utilizing (6),  $\varepsilon_M^l$  can be approximated as [25]

$$\tilde{\varepsilon}_M^l = \begin{cases} 1, & \gamma_M^l \leq p \\ \frac{1}{2} - g\sqrt{N}(\gamma_M^l - h), & p < \gamma_M^l < q \\ 0, & \gamma_M^l \geq q. \end{cases} \quad (25)$$

Using (5) and (25), the average block error rate is expressed as

$$E[\tilde{\varepsilon}_M^l] = \int_0^\infty \tilde{\varepsilon}_M^l(\rho_R x) f_{\sum_{j=1}^l |h_U^j|^2}(x) dx, \quad (26)$$

where  $f_{\sum_{j=1}^l |h_U^j|^2}(x) = \left(\frac{m_U}{\Omega_U}\right)^{m_U l} \frac{x^{m_U l-1}}{\Gamma(m_U l)} e^{-\frac{m_U x}{\Omega_U}}$  is the PDF of  $\sum_{j=1}^l |h_U^j|^2$ .

According to (25),  $E[\tilde{\varepsilon}_M^l]$  can be further expressed as

$$E[\tilde{\varepsilon}_M^l] = \int_{\frac{p}{\rho_R}}^{\frac{q}{\rho_R}} \left(\frac{1}{2} - g\sqrt{N}(\rho_R x - h)\right) f_{\sum_{j=1}^l |h_U^j|^2}(x) dx + \int_0^{\frac{p}{\rho_R}} f_{\sum_{j=1}^l |h_U^j|^2}(x) dx. \quad (27)$$

Substituting the PDF of  $\sum_{j=1}^l |h_U^j|^2$  into (23), which can be expressed as

$$E[\tilde{\varepsilon}_M^l] = \left(\frac{1}{2} + g\sqrt{N}h\right) F_{\sum_{j=1}^l |h_U^j|^2}\left(\frac{q}{\rho_R}\right) + \left(\frac{1}{2} - g\sqrt{N}h\right) F_{\sum_{j=1}^l |h_U^j|^2}\left(\frac{p}{\rho_R}\right) - \left(\frac{m_U}{\Omega_U}\right)^{m_U l} \frac{g\sqrt{N}}{\Gamma(m_U l)} \times \rho_R \left( \int_0^{\frac{q}{\rho_R}} x^{m_U l} e^{-\frac{m_U x}{\Omega_U}} dx - \int_0^{\frac{p}{\rho_R}} x^{m_U l} e^{-\frac{m_U x}{\Omega_U}} dx \right). \quad (28)$$

Utilizing [39, eq.(3.351.1)],  $E[\tilde{\varepsilon}_M^l]$  is derived as (16).

**REFERENCES**

- [1] M. Shirvanimoghaddam, M. Condoluci, M. Dohler, and S. J. Johnson, "On the fundamental limits of random non-orthogonal multiple access in cellular massive IoT," *IEEE J. Sel. Areas Commun.*, vol. 35, no. 10, pp. 2238–2252, Oct. 2017.
- [2] A. Mukherjee, "Physical-layer security in the Internet of Things: Sensing and communication confidentiality under resource constraints," *Proc. IEEE*, vol. 103, no. 10, pp. 1747–1761, Oct. 2015.
- [3] Y. Qu, S. Yu, W. Zhou, S. Peng, G. Wang, and K. Xiao, "Privacy of things: Emerging challenges and opportunities in wireless Internet of Things," *IEEE Wireless Commun.*, vol. 25, no. 6, pp. 91–97, Dec. 2018.
- [4] M. Chen, Y. Miao, Y. Hao, and K. Hwang, "Narrow band Internet of Things," *IEEE Access*, vol. 5, pp. 20557–20577, 2017.
- [5] S. Han, X. Xu, S. Fang, Y. Sun, Y. Cao, X. Tao, and P. Zhang, "Energy efficient secure computation offloading in NOMA-based mMTC networks for IoT," *IEEE Internet Things J.*, vol. 6, no. 3, pp. 5674–5690, Jun. 2019.
- [6] Z. Xiang, W. Yang, Y. Cai, Z. Ding, Y. Song, and Y. Zou, "NOMA assisted secure short-packet communications in IoT," *IEEE Wireless Commun.*, Aug. 2020, doi: 10.1109/MWC.01.1900529.
- [7] M. Alkhatrah, Y. Gong, G. Chen, S. Lambotharan, and J. A. Chambers, "Buffer-aided relay selection for cooperative NOMA in the Internet of Things," *IEEE Internet Things J.*, vol. 6, no. 3, pp. 5722–5731, Jun. 2019.



- [8] Z. Xiang, W. Yang, G. Pan, Y. Cai, and Y. Song, "Physical layer security in cognitive radio inspired NOMA network," *IEEE J. Sel. Topics Signal Process.*, vol. 13, no. 3, pp. 700–714, Jun. 2019.
- [9] D. Chen, W. Yang, J. Hu, Y. Cai, and X. Tang, "Energy-efficient secure transmission design for the Internet of Things with an untrusted relay," *IEEE Access*, vol. 6, pp. 11862–11870, 2018.
- [10] X. Liu and N. Ansari, "Green relay assisted D2D communications with dual batteries in heterogeneous cellular networks for IoT," *IEEE Internet Things J.*, vol. 4, no. 5, pp. 1707–1715, Oct. 2017.
- [11] C. Zhang, J. Ge, M. Pan, F. Gong, and J. Men, "One stone two birds: A joint thing and relay selection for diverse IoT networks," *IEEE Trans. Veh. Technol.*, vol. 67, no. 6, pp. 5424–5434, Jun. 2018.
- [12] V. N. Vo, C. So-In, H. Tran, D.-D. Tran, S. Heng, P. Aimtongkham, and A.-N. Nguyen, "On security and throughput for energy harvesting untrusted relays in IoT systems using NOMA," *IEEE Access*, vol. 7, pp. 149341–149354, 2019.
- [13] G. Shabbir, J. Ahmad, W. Raza, Y. Amin, A. Akram, J. Loo, and H. Tenhunen, "Buffer-aided successive relay selection scheme for energy harvesting IoT networks," *IEEE Access*, vol. 7, pp. 36246–36258, 2019.
- [14] S. Han, X. Xu, Z. Liu, P. Xiao, K. Moessner, X. Tao, and P. Zhang, "Energy-efficient short packet communications for uplink NOMA-based massive MTC networks," *IEEE Trans. Veh. Technol.*, vol. 68, no. 12, pp. 12066–12078, Dec. 2019.
- [15] J. Zeng, T. Lv, Z. Lin, R. P. Liu, J. Mei, W. Ni, and Y. J. Guo, "Achieving ultrareliable and low-latency communications in IoT by FD-SCMA," *IEEE Internet Things J.*, vol. 7, no. 1, pp. 363–378, Jan. 2020.
- [16] Z. Xiang, W. Yang, Y. Cai, J. Xiong, Z. Ding, and Y. Song, "Secure transmission in a NOMA assisted IoT network with diversified communication requirements," *IEEE Internet Things J.*, early access, May 19, 2020, doi: 10.1109/JIOT.2020.2995609.
- [17] J. Chen, L. Zhang, Y.-C. Liang, X. Kang, and R. Zhang, "Resource allocation for wireless-powered IoT networks with short packet communication," *IEEE Trans. Wireless Commun.*, vol. 18, no. 2, pp. 1447–1461, Feb. 2019.
- [18] T. Kim and I. Bang, "An enhanced random access with preamble-assisted short-packet transmissions for cellular IoT communications," *IEEE Commun. Lett.*, vol. 23, no. 6, pp. 1081–1084, Jun. 2019.
- [19] J. Wu, W. Kim, and B. Shim, "Pilot-less one-shot sparse coding for short packet-based machine-type communications," *IEEE Trans. Veh. Technol.*, vol. 69, no. 8, pp. 9117–9120, Aug. 2020.
- [20] L. Zhang and Y.-C. Liang, "Average throughput analysis and optimization in cooperative IoT networks with short packet communication," *IEEE Trans. Veh. Technol.*, vol. 67, no. 12, pp. 11549–11562, Dec. 2018.
- [21] Y. Hu, Y. Zhu, M. C. Gursoy, and A. Schmeink, "SWIPT-enabled relaying in IoT networks operating with finite blocklength codes," *IEEE J. Sel. Areas Commun.*, vol. 37, no. 1, pp. 74–88, Jan. 2019.
- [22] Y. Hu, A. Schmeink, and J. Gross, "Blocklength-limited performance of relaying under quasi-static Rayleigh channels," *IEEE Trans. Wireless Commun.*, vol. 15, no. 7, pp. 4548–4558, Jul. 2016.
- [23] M. Haghifam, B. Makki, M. Nasiri-Kenari, T. Svensson, and M. Zorzi, "Wireless-powered relaying with finite block-length codes," 2016, *arXiv:1611.05995*. [Online]. Available: <http://arxiv.org/abs/1611.05995>
- [24] J. Qi and S. Aissa, "Cross-layer design for multiuser MIMO MRC systems with feedback constraints," *IEEE Trans. Veh. Technol.*, vol. 58, no. 7, pp. 3347–3360, Sep. 2009.
- [25] B. Makki, T. Svensson, and M. Zorzi, "Finite block-length analysis of the incremental redundancy HARQ," *IEEE Wireless Commun. Lett.*, vol. 3, no. 5, pp. 529–532, Oct. 2014.
- [26] B. Makki, T. Svensson, and M. Zorzi, "Wireless energy and information transmission using feedback: Infinite and finite block-length analysis," *IEEE Trans. Commun.*, vol. 64, no. 12, pp. 5304–5318, Dec. 2016.
- [27] B. Makki, T. Svensson, G. Caire, and M. Zorzi, "Fast HARQ over finite blocklength codes: A technique for low-latency reliable communication," *IEEE Trans. Wireless Commun.*, vol. 18, no. 1, pp. 194–209, Jan. 2019.
- [28] Z. Shi, S. Ma, H. ElSawy, G. Yang, and M.-S. Alouini, "Cooperative HARQ-assisted NOMA scheme in large-scale D2D networks," *IEEE Trans. Commun.*, vol. 66, no. 9, pp. 4286–4302, Sep. 2018.
- [29] X. Guan, Y. Cai, and W. Yang, "On the reliability-security tradeoff and secrecy throughput in cooperative ARQ," *IEEE Commun. Lett.*, vol. 18, no. 3, pp. 479–482, Mar. 2014.
- [30] H.-M. Wang, Q. Yang, Z. Ding, and H. V. Poor, "Secure short-packet communications for mission-critical IoT applications," *IEEE Trans. Wireless Commun.*, vol. 18, no. 5, pp. 2565–2578, May 2019.
- [31] Z. Xiang, W. Yang, G. Pan, Y. Cai, and X. Sun, "Secure transmission in non-orthogonal multiple access networks with an untrusted relay," *IEEE Wireless Commun. Lett.*, vol. 8, no. 3, pp. 905–908, Jun. 2019.
- [32] Z. Xiang, W. Yang, G. Pan, Y. Cai, Y. Song, and Y. Zou, "Secure transmission in HARQ-assisted non-orthogonal multiple access networks," *IEEE Trans. Inf. Forensics Security*, vol. 15, pp. 2171–2182, 2020.
- [33] Z. Xiang, W. Yang, Y. Cai, Z. Ding, and Y. Song, "Secure transmission design in HARQ assisted cognitive NOMA networks," *IEEE Trans. Inf. Forensics Security*, vol. 15, pp. 2528–2541, 2020.
- [34] Y. Song, W. Yang, Z. Xiang, N. Sha, H. Wang, and Y. Yang, "An analysis on secure millimeter wave NOMA communications in cognitive radio networks," *IEEE Access*, vol. 8, pp. 78965–78978, 2020.
- [35] Y. Polyanskiy, H. V. Poor, and S. Verdú, "Channel coding rate in the finite blocklength regime," *IEEE Trans. Inf. Theory*, vol. 56, no. 5, pp. 2307–2359, May 2010.
- [36] D. Tuninetti, "On the benefits of partial channel state information for repetition protocols in block fading channels," *IEEE Trans. Inf. Theory*, vol. 57, no. 8, pp. 5036–5053, Aug. 2011.
- [37] Y. Song, W. Yang, X. Yang, Z. Xiang, and B. Wang, "Physical layer security in cognitive millimeter wave networks," *IEEE Access*, vol. 7, pp. 109162–109180, 2019.
- [38] Y. Song, W. Yang, Z. Xiang, B. Wang, and Y. Cai, "Secure transmission in mmWave NOMA networks with cognitive power allocation," *IEEE Access*, vol. 7, pp. 76104–76119, 2019.
- [39] I. S. Gradshteyn and I. M. Ryzhik, *Table of Integral, Series and Products*, 7th ed. New York, NY, USA: Academic, 2007.



**YUCUI YANG** received the M.S. degree from the College of Automation Engineering, Nanjing University of Aeronautics and Astronautics, Nanjing, in 2006. She is currently with the School of Physics and Electronic Electrical Engineering, Huaiyin Normal University. She is also with the Jiangsu Province Key Construction Laboratory of Modern Measurement Technology and Intelligent System. Her current research interests include cooperative communications, pattern recognition, and image retrieval.



**YI SONG** received the M.S. degree from the Nanjing University of Aeronautics and Astronautics, in 2011. He is currently pursuing the Ph.D. degree with the Institute of Communications Engineering, Army Engineering University of PLA. His research interests include millimeter-wave, non-orthogonal multiple access, physical-layer security, and cognitive radio.



**FENGLIAN CAO** received the M.S. degree from the School of Electronic Science and Engineering, Nanjing University, Nanjing, in 2006. She is currently with the School of Physics and Electronic Electrical Engineering, Huaiyin Normal University. Her current research interests include cooperative communications, non-orthogonal multiple access, and physical-layer security.